IPNO/TH 95-44

IFUP-TH 39/95

NEUTRON BREAKUP IN PERIPHERAL HEAVY-ION COLLISIONS: REACTIONS INDUCED BY ^{11}Be

Angela Bonaccorso*

Division de Physique Théorique,

Institut de Physique Nuclèaire, IN2P3-CNRS, 91406 Orsay, Cedex, France.

and

*Istituto Nazionale di Fisica Nucleare, Sezione di Pisa, 56100 Pisa, Italy**

and

D.M.Brink

Dipartimento di Fisica, Università di Trento,38050 Povo,Italy

UNIVERSITÀ DEGLI STUDI DI PISA

DIPARTIMENTO DI FISICA

Istituto Nazionale di Fisica Nucleare

Sezione di Pisa

Abstract

In this paper we study the neutron breakup in the reaction $^9Be(^{11}Be,^{10}Be)^9Be + n$ at $E_{inc} = 41A.MeV$. The neutron angular distribution is obtained from a general formalism which can be applied to any heavy-ion transfer to the continuum reaction at intermediate energies. The characteristics of the asymptotic part of the neutron wave function in ^{11}Be are discussed in detail. Our theoretical results for the angular distribution and for the total breakup cross section are compared to recent experimental data. We give also some qualitative estimates of the 2n-breakup cross section in ^{11}Li-induced reactions.

PACS number(s):25.70.Hi,25.70Mn

* Permanent Address

E-mail: Decnet 39186::BONAC ; Internet BONAC@IBMTH.DIFI.UNIPI.IT

I. INTRODUCTION

A large number of heavy-ion reactions at intermediate and high energies have shown that the breakup of light particles from the projectile is at the origin of a relevant part of the cross section due to the peripheral collisions. According to the framework in which these particles are found they have been called pre-equilibrium particles (cf.fragmentation reactions), 3-body physical background (transfer to the continuum reactions), halo-neutron breakup (reactions with exotics beams). This component of the cross section can be determined experimentally from exclusive mesurements of the light particle in coincidence with the ejectile.

One of the aim of this paper and of a forthcoming one, which we will refer to as I and II respectively, is to show that models developed in Refs. [1,2] to study breakup and transfer

to the continuum in heavy-ion reactions, which are peripheral processes dominated by the overlap of the tails of the neutron wave-functions in the initial and final state [1], are well suited to study neutron breakup in several of the above mentioned cases.

Furthermore we will show that besides the energy spectra, we can also calculate the angular distribution of the breakup neutrons. This is of particular interest for the understanding of the mechanism of halo-nucleus induced reactions as discussed in [3] but it is important also for the analysis of exclusive experiments in one-neutron transfer to the continuum reactions [4–6] where the breakup neutrons need to be distinguished from the neutrons coming from the decay of the target resonance states populated by transfer.

In previous works we have shown that the transfer to the continuum cross section is due to the sum of absorption on resonant and non resonant states of the target, and elastic breakup. The relative importance of the two processes depends on the projectile-target combination and on the incident energy. In Ref. [7] we argued that reactions initiated by a nucleus having a weekly bound neutron should be dominated by the elastic breakup process. The same happens when the target does not have narrow single particle resonance states in the continuum which can be populated by transfer. Our model does not contain the effect of the Coulomb breakup. Therefore it can be used only to calculate the nuclear breakup.

This paper is concerned in particular with direct reactions induced by halo nuclei like ^{11}Be. This nucleus has a very loosely bound neutron whose single-particle $2s_{1/2}$ wave function has a long tail. Peripheral reactions induced by a halo nucleus will have characteristics similar to those of other heavy-ions, but in a more extreme form because of the very weak binding of the halo nucleons. For comparison we will show also some results of a ^{10}Be breakup reaction.

The paper is organized as it follows. Section II contains the formalism, and its physical interpretation, for the neutron angular distribution obtained from the breakup amplitude given in Ref. [2]. The formula has the form of a convolution integral typical of diffraction and therefore contains all possible mechanisms for the production of free neutrons. The integral

can be calculated analytically by making simple approximations thus giving an explicit form for the angular distribution.

In Section III we discuss the asymptotic normalization constant of the initial state wave function and the corresponding momentum distribution. Section IV is devoted to the analysis of the reaction $^9Be(^{11}Be,^{10}Be)^9Be + n$ at $E_{inc} = 41A.MeV$, which has been studied experimentally [3]. In Section V we give some qualitative estimates of the 2n-breakup cross section in ^{11}Li-induced reactions. Section VI contains our conclusions.

In a forthcoming paper we will study the breakup part of the reaction $^{48}Ca(^{20}Ne,^{19}Ne)^{49}Ca$ at $E_{inc} = 48A.MeV$ [5,6].

II. NEUTRON ANGULAR DISTRIBUTION

In equation (3.1) of Ref. [2] we gave the expression for the transition amplitude corresponding to the break-up of a neutron from the projectile in a heavy-ion reaction. It was calculated by time dependent perturbation theory taking as initial state the single particle wave function of the neutron bound in the projectile and as final state a plane wave of definite momentum $|\mathbf{k}_f| = 2m\varepsilon_f/\hbar^2$ where ε_f is the neutron free-particle energy after the breakup. We worked in a reference frame which has the origin at the center of the target, the x-axis along the distance of closest approach between the two nuclei and the z-axis along the direction of relative motion. Then the initial state wave function in the moving potential is obtained by a Galilean transformation of the wave function calculated in the projectile rest frame [8]. The core of the halo nucleus is assumed to move on a straight line trajectory with impact parameter $\mathbf{d}$ which is in the direction of the x-axis.

The breakup transition amplitude can be written as

$$A_{01} = \frac{1}{i\hbar}\int_{-\infty}^{+\infty} dt \int_{-\infty}^{+\infty} dxdydz e^{-i\mathbf{k}_f\cdot\mathbf{r}}\, V_2(\mathbf{r})\, \psi_1(|x-d|,y,z-vt) e^{\frac{i}{\hbar}(mvz+(\varepsilon_f-\varepsilon_1+\frac{1}{2}mv^2)t)}$$
$$= \frac{i}{\hbar v}\int dxdy \int dzdz' e^{ik_2 z} e^{-i\mathbf{k}_f\cdot\mathbf{r}} V_2(\mathbf{r}) e^{-ik_1 z'} \psi_1(|x-d|,y,z')$$

$$= \frac{i}{\hbar v} \int dxdy \int dz \tilde{\psi}_1(|x-d|, y, k_1) e^{ik_2 z} e^{-i\mathbf{k}_f \cdot \mathbf{r}} V_2(\mathbf{r}) \tag{2.1}$$

where k_1 and k_2 are given by

$$k_1 = -\frac{\varepsilon_i - \varepsilon_f + \frac{1}{2}mv^2}{\hbar v} \qquad k_2 = -\frac{\varepsilon_i - \varepsilon_f - \frac{1}{2}mv^2}{\hbar v}. \tag{2.2}$$

To calculate analytically the angular distribution we proceed in the following way. First we calculate the integral over z and z' and obtain the Fourier transform with respect to the z dependence of V_2 and ψ_1

$$A_{01}(\mathbf{k_f}) = \frac{1}{iv\hbar} \int d\mathbf{b} \exp(-i\mathbf{k}_\perp \cdot \mathbf{b}) \tilde{V}_2(\mathbf{b}, k_z - k_2) \tilde{\psi}_1(\mathbf{d} - \mathbf{b}, k_1). \tag{2.3}$$

where $\mathbf{b}$ is the projection of the neutron position vector $\mathbf{r}$ on the (x,y) plane, $\mathbf{k_f}$ is the momentum of the emitted neutron, k_z is the z-component of $\mathbf{k_f}$, $\mathbf{k}_\perp$ is the component of $\mathbf{k_f}$ parallel to the (x,y)-plane.

Eq. (2.3) is very interesting because it has the form of a Fourier transform integral characteristic of diffraction phenomena [9]. In particular it represents the convolution of the potential of the target with the wave function of the initial state. Therefore we expect Eq.(2.3) to give rise to a diffractive-like angular distribution. The initial state wave function can be interpreted as an amplitude function and the potential as a transmission function. The region in which these two functions have an overlap different from zero is very small, in fact it has the dimensions of the overlap region between the two nuclei at the instant of transfer, therefore the resulting diffraction pattern will have a large spread around the incident direction.

Equation (2.3) can be simplified by using approximate forms for the functions $\tilde{V}$ and $\tilde{\psi}$. From the appendix to Ref. [10] we have

$$\tilde{\psi}_{l_1 m_1}(\mathbf{d} - \mathbf{b}, k_1) \approx C_1 Y_{l_1 m_1}(\hat{\mathbf{k}_1}) e^{-\eta\rho} \left(\frac{2\pi}{\eta\rho}\right)^{\frac{1}{2}} \tag{2.4}$$

$\tilde{\psi}$ is the Fourier transform of the asymptotic part of the initial state wave function which is discussed in detail in the next section. In Eq.(2.4) $\rho = |(\mathbf{d} - \mathbf{b})|$ and

$$\eta^2 = k_2^2 - k_f^2 = k_1^2 + \gamma_i^2. \tag{2.5}$$

where $\gamma_i = \sqrt{-2m\varepsilon_i}/\hbar$ and ε_i is the initial bound state energy. We use a surface approximation to $V_2(r)$ given by

$$V_2(r) = V_2(b)e^{-\frac{z^2}{2ab}} \tag{2.6}$$

where

$$b = (x^2 + y^2)^{\frac{1}{2}} \qquad \text{and} \qquad V_2(b) = \frac{V_0}{1 + e^{\frac{(b-R_2)}{a}}} \tag{2.7}$$

The Fourier transform of (2.6) is given by

$$\tilde{V}_2(b, k_z - k_2) = V_2(b)e^{-(k_z-k_2)^2\frac{ab}{2}}(2\pi ab)^{\frac{1}{2}} \tag{2.8}$$

Using Eq.(2.4) and Eq.(2.8) in Eq.(2.3) we obtain

$$|A_{01}(\mathbf{k_f})|^2 = F(k_f)|I(k_f)|^2 \tag{2.9}$$

Where

$$F(k_f) = \frac{|C_1|^2}{\hbar^2 v^2}\frac{\pi a}{\eta}\frac{R_2}{R_1}V_0^2 P_{l_1}(X_1)e^{-(k_z-k_2)^2 aR_2} \tag{2.10}$$

and

$$|I(k_f)|^2 = \left|\int_0^\infty d\mathbf{b}\; e^{-i\mathbf{k}_\perp\cdot\mathbf{b}}\frac{e^{-\eta|\rho|}}{1 + e^{(\mathbf{b}-R_2)/a}}\right|^2 \tag{2.11}$$

Equation (2.9) was obtained by approximating the slowly varying factors in the integral

$$\left(\frac{\mathbf{b}}{\mathbf{b}-\mathbf{d}}\right)^{\frac{1}{2}} \approx \frac{R_2}{R_1} \qquad \text{and} \qquad e^{-(k_z-k_2)^2\frac{ab}{2}} \approx e^{-(k_z-k_2)^2 aR_2/2} \tag{2.12}$$

and using

$$\frac{1}{2l_1+1}\sum_{m_1}|Y_{l_1 m_1}|^2 = P_{l_1}(X_1)/4\pi \tag{2.13}$$

where $X_1 = 1 + 2k_1^2\gamma_i^2$. The integrand in Eq. (2.11) is peaked near $b = R_2$ therefore ρ can be approximated as

$$\rho = |(\mathbf{d} - \mathbf{b})| = \sqrt{(d-x)^2 + y^2} = (d-x)\sqrt{1 + \frac{y^2}{(d-x)^2}} \approx (d-x) + \frac{y^2}{2(d-R_2)} \tag{2.14}$$

then

$$e^{-\eta|\rho|} \sim e^{-\eta d} e^{\eta x} e^{-\eta \frac{y^2}{2R_1}}. \tag{2.15}$$

Finally

$$\begin{aligned} I(k_f) &\approx e^{-\eta d} \int_{-\infty}^{\infty} dy\ e^{-ik_y y} e^{-\frac{\eta}{2R_1} y^2} \int_{-\infty}^{\infty} dx\ e^{-ik_x x} \frac{e^{\eta x}}{1 + e^{(x-R_2)/a}} \\ &= e^{-\eta d} (2\pi R_1/\eta)^{\frac{1}{2}} e^{(\eta - ik_x)R_2} e^{-\frac{R_1}{2\eta} k_y^2} \int_{-\infty}^{\infty} d\bar{x}\ \frac{e^{(\eta - ik_x)\bar{x}}}{1 + e^{\bar{x}/a}} \\ &= e^{-\eta(d-R_2)} (2\pi R_1/\eta)^{\frac{1}{2}} e^{-ik_x R_2} e^{-\frac{d}{2\eta} k_y^2} \frac{\pi a}{\sin((\eta - ik_x)a\pi)} \end{aligned} \tag{2.16}$$

The justification for the above approximation is that the integrand is different from zero only in a limited region of space given by the overlap of the two nuclei at the instant of transfer. This region is larger in y-dimension than in x-dimension. The x-integration has been extended from zero to ∞ because the integrand is large only on the surface region of the target. From equation (2.16) we get

$$|I(k_f)|^2 \approx \frac{2\pi^3 a^2 R_1}{\eta} e^{-\frac{R_1}{\eta} k_y^2} \frac{e^{-2\eta(d-R_2)}}{\cosh(2k_x a\pi) - \cos(2\eta a\pi)} \tag{2.17}$$

In the above equations $\mathbf{k_f}$ is the momentum of the emitted neutron whose components are

$$k_x = k_f \sin\theta \cos\phi \tag{2.18}$$

$$k_y = k_f \sin\theta \sin\phi \tag{2.19}$$

$$k_z = k_f \cos\theta \tag{2.20}$$

One obtains then for the square of the transition amplitude

$$|A_{01}(\mathbf{k_f})|^2 = Ce^{-\frac{R_1}{\eta}k_f^2 \sin^2\theta \sin^2\phi} \frac{e^{-(k_f \cos\theta - k_2)^2 a R_2}}{\cosh(2k_f a\pi \sin\theta\cos\phi) - \cos(2\eta a\pi)} \tag{2.21}$$

Where

$$C = \frac{|C_1|^2}{\hbar^2 v^2} 2\pi^4 a^3 R_2 V_0^2 \frac{P_{l_1}(X_1)}{\eta^2} e^{-2\eta(d-R_2)} \tag{2.22}$$

In equation (2.21) ϕ is the angle between $\mathbf{k}_\perp$ and the x-axis. The term $e^{-\frac{R_1}{\eta}k_f^2 \sin^2\theta \sin^2\phi}$ can be approximated by a δ-function as

$$e^{-\beta^2 \sin^2\phi} = A(\delta(\phi) + \delta(\pi - \phi)) \tag{2.23}$$

where

$$\beta^2 = \frac{R_1}{\eta} k_f^2 \sin\theta^2. \tag{2.24}$$

$$\begin{aligned} A &= \frac{1}{2}\int_0^{2\pi} d\phi e^{-\beta^2 \sin^2\phi} \\ &= e^{-\beta^2/2} \int_0^{2\pi} e^{\frac{\beta^2}{2}\cos\phi}\, d\phi \\ &= 2\pi e^{-\beta^2/2} J_0(i\beta^2/2) \\ &= 2\pi e^{-\beta^2/2} I_0(\beta^2/2) \end{aligned} \tag{2.25}$$

Where J_0 and I_0 are Bessel functions [11], and we used the integral representation of J_0 (ibidem eq.8.411,7 pag .953).

The physical meaning of Eq.(2.25) is that the neutron is emitted in (or near) the reaction plane. The δ-function approximation is not valid at very forward angles because $\sin\theta \sim 0$ and β is very small, but in this region the out-of-plane contribution would be negligible anyway.

In Ref. [2] the total breakup probability was given as

$$P_{breakup} = \frac{1}{8\pi^3} \int d\mathbf{k}_\perp dk_z |A_{01}(\mathbf{k_f})|^2 \tag{2.26}$$

The double differential probability spectrum can be obtained from the above equation as

$$\frac{dP^2_{breakup}}{d\varepsilon_f d\Omega} = \frac{1}{8\pi^3} k_f^2 \frac{dk_f}{d\varepsilon_f} |A_{01}(\mathbf{k_f})|^2$$
$$= BF(\theta) \tag{2.27}$$

Where

$$F(\theta) = \frac{e^{-k_f^2 a R_2 (\cos\theta - k_2/k_f)^2} e^{-\frac{R_1}{2\eta} k_f^2 \sin^2(\theta)}}{\cosh(2a\pi k_f \sin\theta) - \cos(2\eta a\pi)} I_0(\beta^2/2) \tag{2.28}$$

and

$$B = \frac{1}{8\pi^3} k_f^2 \frac{m}{\hbar^2 k_f} C$$
$$= \frac{m\pi |C_1|^2}{4\hbar^4 v^2} k_f \frac{a^3}{\eta^2} R_2 V_0^2 P_{l_1}(X_1) e^{-2\eta(d-R_2)} \tag{2.29}$$

The above formulas have been obtained in the case of a real interaction potential $V_2(r)$ between the neutron and the taget. The generalization to the case of a complex potential is obtained by substituting in the expression for B, V_0^2 with $V_0^2 + W_0^2$ where W_0 is the strength of the imaginary potential. Usually the effect of the imaginary potential on the elastic breakup is very small as its strength is about one order of magnitude smaller than the strength of the real potential.

The form of the angular distribution is very simple and interesting to discuss. The term indicated as B contains the dependence on the numerical and geometrical parameters of the reactions in a very staightforward way. There is a rather strong a^3 dependence on the target potential diffuseness. It is in a sense obvious as diffraction effects are very sensitive to the sharpness of the diffractive surface. It is reminiscent of the so called Nemets effect [17,18] of deuteron breakup where it was found that the breakup cross sections varied a lot if the target changed from a closed shell to a non closed shell nucleus. The dependence on the asymptotic normalization constant C_1 of the initial state will be discussed in detail in the

next section. Then there is the exponential term which depends on the difference between the distance of closest approach and the target radius. This term partially determines the magnitude of the cross section as discussed in Section IV.

Also the dependence on the value of η, defined by Eq.(2.5), is very important. A special feature of the ^{11}Be induced reactions is that the neutron binding energy, $\varepsilon_i = -0.5MeV$ is much smaller than for most other cases. The value of $\gamma_i = 0.155fm^{-1}$ is also very small. This makes the breakup cross section large and gives other features which will be discussed later on in this paper. The values of the parameter η as a function of the final energy ε_f are shown in Fig.(1) for the case of ^{11}Be by the solid line. Also shown is the same parameter for a ^{10}Be projectile (dashed line) whose last neutron binding energy is $\varepsilon_i = -6.8MeV$. There is a much stronger energy dependence and the minimum value of η is much smaller in the case of ^{11}Be .

The term $F(\theta)$ contains all the angular dependence and also the energy-momentum matching conditions. The source of the neutrons is in the overlap region. In a normal diffraction the source is some arrangement of slits and it is two-dimensional. In our case it is three-dimensional. It is a kind of cigar shaped region and Eq.(2.28) results from the Fourier transform of the amplitude in that region. In Eq. (2.28) the first term comes from the transform in the z-direction the second term comes from the y-direction perpendicular to the reaction plane, and the denominator comes from the x-direction. The two terms $e^{-\frac{R_1}{2\eta}k_f^2\sin^2(\theta)}$ and $I_0(\beta^2/2)$ compensate each other almost exacly because $\beta^2/2$ is not too large.

Then the form of the angular distribution is given just by the oscillating term in the denominator multiplied by the exponential term $e^{-k_f^2 aR_2(\cos\theta - k_2/k_f)^2}$ which comes from the Fourier transform of the target potential. The relative behaviour of these two terms is important to determine whether or not the angular distribution will have a secondary maximum at $\theta = \pi$. In principle this is possible if the decay of the exponential term is not too fast because the denominator gives a maximum at $\theta = 0$ and $\theta = \pi$.

In Fig.(6) we show the behaviour of the term $e^{-k_f^2 aR_2(\cos\theta - k_2/k_f)^2}$ and of the term $\frac{1}{\cosh(2k_f a\pi \sin\theta) - \cos(2\eta a\pi)}$ in Eq.(19) for the ^{11}Be breakup (solid line and dashed line respectively), and for the ^{10}Be breakup (dotdashed line and dotted line respectively), for a final neutron energy $\varepsilon_f = 40MeV$.

Finally we make some remarks on how our formula can be used to make comparison with experimental data. We have seen that the dependence on ϕ is very close to a δ- function which means the neutrons are emitted preferentially on the reaction plane. The direction of the momentum of the ejectile does not appear in our formulas and this corresponds to experimental data in which one integrates on the direction of the ejectile. However it is important to notice that all the reactions we mentioned in the introduction, for which neutron breakup is important, show ejectile angular distributions which are structurless and peaked in the forward direction. It is worth mentioning also that in several experimental papers the light particle breakup from the projectile is often called the "uncorrelated component" because its behaviour does not depend on the angle of detection of the ejectile.

The probability distribution Eq.(2.27) is appropriate for a situation where the final state of the neutron is specified by its energy and angle of emission. The final state can also be specified by giving the transverse ($k_\perp$) and longitudinal (k_z) components of the neutron momentum. Then the probability distribution follows directly from Eq.(2.26) as

$$\frac{dP^2_{breakup}}{dk_\perp dk_z} = \frac{1}{8\pi^3} k_f^2 \frac{dk_f}{d\varepsilon_f} |A_{01}(k_\perp, k_z)|^2 \tag{2.30}$$

III. APPLICATION TO ^{11}BE-INDUCED REACTIONS

A. Asymptotic wave function and normalization constant

The breakup amplitude Eq.(2.3) depends on the Fourier transform of the asymptotic part of the initial state wave function. The single particle wave function for the initial state is

$$\psi(\mathbf{r}) = \frac{\phi(r)}{r} Y_{lm}(\Omega) \tag{3.1}$$

normalized such that $\int |\phi(r)|^2 dr = 1$. According to Refs. [1,12] the asymptotic part of Eq.(3.1) is given in terms of Hankel functions by

$$\phi(r)/r = C_1 \ \gamma_i \ h_l^{(+)}(i\gamma_i r) \qquad at \qquad r \to \infty \tag{3.2}$$

where γ_i was defined after Eq.(2.5). C_1 does not give the normalization of the full wave function Eq.(3.1) but it is defined in terms of it as

$$C_1 = \frac{\phi(r)}{r\gamma_i h_l^{(+)}(i\gamma_i r)} \qquad at \qquad r \to \infty \tag{3.3}$$

Usually an accurate way to find C_1 is to solve numerically the Schrödinger equation for $\phi(r)/r$ with the requirement that it should have the correct values of the bound state parameters ε_i, l, m and then to match it onto the corresponding Hankel function according to Eq.(3.3). It is also possible to find an analytical form for C_1 using the WKB form of the wave function [13,14]. The formula obtained in [13] in the case $l = 0$ which is relevant for the $^{11}Be \ \ 2s_{1/2}$ wave function is

$$C_1^2 = \frac{m}{\gamma_i \hbar} \frac{1}{T} e^{2\gamma_i R} \tag{3.4}$$

where T is the classical period of the particle in the potential pocket [16], $R = 2.6fm$ is the radius of the nucleus. In this case $T = 2.8 \ 10^{-22} sec$, then a reasonable estimate is $C_1 \simeq 0.94 fm^{-1/2}$.

Values of the constant C_1 have also been calculated by a numerical solution of the radial Schrödinger equation corresponding to Woods-Saxon potentials having different sets of parameters which however all give the correct binding energy for the neutron. All the corresponding wave functions are very close to each other on the tail having a value of $|\phi(r)/r|^2 \sim 10^{-4} fm^{-3}$ at $r = 12fm$ and differ only in the innermost part of the potential. The shell model wave function of Sagawa [15] has also the same behaviour. In all the cases we studied we found values of $C_1 = .81 - 1.01 fm^{-1/2}$.

Sometimes, however, the asymptotic form of the wave function is treated in a different way which can lead to a very different effective normalization constant. We think that the asymptotic form of the wave function should be taken to be an Hankel function and the asymptotic normalization constant C_1 should be obtained from a solution of the radial Schrödinger equation as discussed above, possibly modified by a spectroscopic factor as we will discuss in the following section. For example the overall normalization to the data used in the calculations of Ref. [3] would correspond to $C_1 = 0.19 fm^{-1/2}$. This value could be obtained only if $|\phi(r)/r|^2 \sim 10^{-5} fm^{-3}$ at $r = 12 fm$, which means the radial wave-function should be an order of magnitude smaller than those calculated with several standard potentials.

B. Momentum distribution

We have seen in Section II that the breakup amplitude Eq.(2.3) depends explicitly on the momentum distribution of the neutron in the projectile given by Eq.(2.4). It was obtained by an analytical calculation of the Fourier transform of the asymptotic part of the initial state wave function. We show it in Fig.(3) for the neutron initial $2s_{1/2}$ state in ^{11}Be by the solid line and for the $1p_{3/2}$ state in ^{10}Be by the dashed line. It is interesting to notice the close resamblance between the momentum distribution in Fig.(3) and the angle integrated energy spectra of the breakup neutrons of Fig.(6) which we discuss in detail in the next section.

The momentum distribution is sharper in ^{11}Be than in ^{10}Be. This is due to the lower binding energy and larger neutron radius (cf.Table I). It is also a characteristic of s-state momentum distribution to be narrower than for larger l-values. The larger absolute value of the $1p_{3/2}$ momentum distribution in ^{10}Be is due to the large value of the asymptotic normalization constant.

State	ε_i(MeV)	$\gamma_i(fm^{-1})$	$C_1(fm^{-1/2})$	C^2S	$R_1(fm)$
$^{11}Be\ 2s_{1/2}$	-0.5	0.155	0.94	0.77	6.5
$^{10}Be\ 1p_{3/2}$	-6.8	0.572	1.96	4	2.6
$^{11}Li\ 2s_{1/2}$	-0.125	0.078	0.46	2	4.4—6.4—8.4
$^{11}Li\ 1p_{1/2}$	-0.125	0.078	0.11	2	4.4—6.4—8.4

Table I: Initial-state parameters in ^{11}Be, ^{10}Be, ^{11}Li. For ^{11}Li we give three possible values of the last neutron orbit radius $R_1 = R_s - R_2$ with R_s and R_2 from Table III and Table II respectively.

IV. RESULTS AND DISCUSSION

In this section we analyse the reaction $^9Be(^{11}Be.^{10}Be)^9Be+n$ at $E_{inc} = 41A.MeV$. Due to the low binding energy of the neutron and to the rather high incident energy this reaction is largely dominated by the breakup. For comparison we calculate also the one-neutron breakup of ^{10}Be at the same energy and on the same target.

V_0(MeV)	$a(fm)$	$R_2(fm)$
-52.3	0.4	2.6

Table II: Target potential parameters in ^9Be .

We obtain the cross section in terms of the breakup probability as [1]

$$\sigma_{breakup}(\varepsilon_f,\theta) = C^2S2\pi \int_0^\infty d\mathrm{d}\frac{dP^2_{breakup}}{d\varepsilon_f d\Omega}(d)P_{el}(d)$$
$$= C^2S\pi\frac{R_s}{\eta}\frac{dP^2_{breakup}}{d\varepsilon_f d\Omega}(R_s) \qquad (4.1)$$

where $\frac{\pi R_s}{\eta}$ is a geometrical factor whose value is close to the geometrical cross section and $C^2S = 0.77$ is the experimental spectroscopic factor [3] of the $2s_{1/2}$-state in ^{11}Be. P_{el} is the

probability that the projectile core-target system remains in the ground state during the breakup reaction and we suppose that the strong absorption hypotesis is satisfied such that $P_{el} = 1$ for $d > R_s$ and $P_{el} = 0$ for $d < R_s$. R_s is the strong absorption radius in the ion-ion collision [1].

The expression for $P_{breakup}$ contains a factor $e^{-2\eta(R_s - R_2)}$ which depends on the difference between the strong absorption radius and the target radius. This difference can be regarded as the breakup radius of the traditional theories of deuteron breakup. Its value has a strong influence on the magnitude of the cross section and in our opinion it is also the parameter that it is more difficult to determine from first principles and that could be taken as a fitting parameter in cases like halo nucleus induced reactions. For the general case of heavy-ion reactions one usually takes $R_s = 1.5(A_P^{1/3} + A_T^{1/3})$ [19], where A_P and A_T are the projectile and target mass numbers.

In Fig.(4) we show the neutron angular distribution calculated with the formalism of Section II using the numerical parameter values of Table I. Experimental points from Ref. [3] are also shown. In order to compare to the experimental data we have integrated the enegy spectra in the range $\varepsilon_f = 26 - 80 MeV$. The solid curve has been calculated at a strong absorption radius of $R_s = 9.4 fm$, slightly larger than the sum of the radius of the neutron orbit in the projectile ($R_1 = 6.5 fm$) and of the target ($R_2 = 2.6 fm$) radius. The dotted line is the energy integrated angular distribution of the breakup neutron from ^{10}Be.

In Fig.(5) we show the same numerical result of Fig.(4), for ^{11}Be, over the whole angular range together with the result of the calculation with $a = 0.55 fm$ (close dotted curve) and $a = 0.65 fm$ (dot dashed curve). It is very interesting to notice that the diffuseness parameter of the target potential changes the behaviour at large angles showing that a sharp surface diffracts more than a smooth one.

In Fig.(6) we show the angle integrated energy spectra. solid line for ^{11}Be projectile, dotted line for ^{10}Be projectile. The corresponding total breakup cross section, integrated over energies and angles, is $\sigma_{breakup} = 0.16 barn$ in good agreement we the results of Ref. [3]

for ^{11}Be while for ^{10}Be we obtain $\sigma_{breakup} = 0.027barn$. Also one should notice that the form of the energy spectrum reproduces that of the momentum distribution of the neutron in the projectile given in Fig.(3). The relationship between the momentum scale in Fig.(3) and the energy scale in Fig.(6) is given by Eq.(2.2). Is shows how the dynamics of the reaction modifies the initial momentum distribution .

Finally we would like to comment on the rising of the angular distribution towards $\theta = \pi$ which is somehow surprising as one usually belives that breakup should be only focussed at forward angles. When the condition $\eta^2 < 1/2aR_2$ is satisfied, the function $F(\theta)$ in Eq.(2.28) can have a secondary maximum. Since from Eq.(2.5) the minimum value of $\eta = \gamma_i$, the previous condition can also be written as $1/\gamma_i < \sqrt{2aR_2}$. This is equivalent to the statement that the radius of the halo is larger than $\sqrt{2aR_2}$, since γ_i is a mesure of the halo radius. In this case the maximum at $\theta = \pi$ of the oscillatory term $\frac{1}{\cosh(2a\pi k_f \sin\theta) - \cos(2\eta a\pi)}$ in Eq.(2.28) is not cancelled by the gaussian term $e^{-k_f^2 aR_2(\cos\theta - k_2/k_f)^2}$ (cf.Fig.(2)) .

V. PREDICTIONS ON ^{11}LI-INDUCED REACTIONS

The halo nucleus ^{11}Li has two very weakly bound nucleons. It is not sure whether the dominant structrure is $(s_{1/2})^2$ or $(p_{1/2})^2$. There is a possibility that a breakup reaction could distinguish between these two structures. To obtain a qualitative understanding of the factors involved we assume that the two nucleons are uncorrelated with a binding energy of $\varepsilon_i = -0.125MeV$, equal to one half of the total binding energy of the two halo neutrons. We calculate the breakup cross section for the two cases where the two neutrons are in a (i) $(s_{1/2})^2$ configuration and (ii) a $(p_{1/2})^2$ configuration. The breakup cross section has a sharp peak near the beam energy which can be characterized by giving the total breakup cross section and the width at half peak.

R_s	7	9	11
σ_s	2.206	1.733	1.305
σ_p	0.252	0.180	0.129
Γ_s	4.5	4.0	3.8
Γ_p	7.0	6.4	5.7
σ_s	0.200	0.144	0.104
σ_p	0.026	0.017	0.012
Γ_s	11.2	10	10
Γ_p	18	15.2	15

Table III:Results for the 2n-breakup in ^{11}Li at $E_{inc} = 33A.MeV$ (top) and $E_{inc} = 200A.MeV$ (bottom). Units are: R_s in fm, 2n-breakup cross section in barn, widths at half maximum of the 0^o-energy distribution in MeV.

We show results at two incident energies $E_{inc} = 33A.MeV$ and $E_{inc} = 200A.MeV$ for the reaction $^9Be(^{11}Li.^9Li)^9Be + 2n$. The 2n-breakup cross section calculated from Eq.(35) integrating over angle and energy, depends on the strong absorption radius R_s which is not so well determined from first principles. To see the sensitivity to R_s we calculate for a range of values. The results are given in Table III. The given widths refer to the energy spectrum at $\theta = 0^o$.

The numbers in Table III show that the breakup characteristics are very sensitive to the initial state structure as well as to the strong absorption radius. There is an order of magnitude difference between the $s_{1/2}$ and $p_{1/2}$ total cross sections and about a factor $e^{-2\gamma_i \Delta R_S} = 0.78$ difference when the strong absorption radius decreases by ΔR_s=2fm. Also the width at half maximum for the 0^o-energy spectrum increases by about 50% from the $2s_{1/2}$ to the $1p_{1/2}$ state. We show results at two incident energies $E_{inc} = 33A.MeV$ and $E_{inc} = 200A.MeV$.

VI. CONCLUSIONS

In this paper we have developed a diffractional model to study neutron breakup from the projectile in heavy-ion reactions. Our model provides the neutron angular distribution and energy spectrum. It is obtained from the calculation of the transition amplitude in time dependent perturbation theory. We assume that the initial state of the neutron is given by the asymptotic part of the single particle bound state wave function in the projectile and that the final state is a free particle wave function of given momentum.

The accuracy of the model has been tested by applying it to the study of the reaction $^9Be(^{11}Be,^{10}Be)^9Be+n$ at $E_{inc}=41A.MeV$, which is particulary suited as the last neutron in ^{11}Be is weakly bound and its wave function has a long tail. Comparison with the experimental angular distribution and absolute value of the cross section is good. Furthermore we have suggested that there is some evidence for a rather large breakup radius. Also our calculations show that the angular distribution should have a secondary maximum at $\theta=\pi$. We have interpreted this effect as due to the particular dimension of a halo projectile. If this effect is confirmed by experiment we would have found a new nice method to investigate the halo properties. The breakup of ^{10}Be has also been discussed.

Finally we have presented some qualitative estimates for the 2n-breakup cross section in ^{11}Li-induced reactions.

Acknowledgments

One of us (A.B.) is very grateful to Nicole Vinh Mau for several discussions and to all members of the group *Structure Nuclèaire par Reactions* of the IPN d'Orsay for the warm hospitality during the preparation of this paper.

REFERENCES

[1] A.Bonaccorso and D.M.Brink, Phys. Rev. C**38**, 1776 (1988).

[2] A.Bonaccorso and D.M.Brink, Phys.Rev. C**43**, 299 (1991).

[3] R.Anne et al., Nucl.Phys. **A575**, 25 (1994).

[4] D.Beaumel, S.Fortier, S.Galès , J.Guillot, H.Langevin-Joliot, H.Laurent , J.M.Maison, J.Vernotte, J.Bordewijck, S.Brandenburg, A.Krasznahorkay, G.M.Crawley, C.P.Massolo and M.Renteria , Phys. Rev. C**49**, 2444 (1994).

[5] H.Laurent, D.Beaumel, S.Fortier, S.Galès, I.Lhenry, J.M.Maison, Y.Blumenfeld, N.Frascaria, J.Guillot, J.C.Roynette, J.A.Scarpaci, T.Suomijärvi, A.Gillibert, IPNO-DRE preprint July 1995.

[6] H.Laurent, D.Beaumel, S.Fortier, S.Galès, I.Lhenry, J.M.Maison, Y.Blumenfeld, N.Frascaria, J.Guillot, J.C.Roynette, J.A.Scarpaci, T.Suomijärvi, A.Gillibert, Contributions to the ' N-N Collisions V Conference', Taormina, Italy, 1994. Edited by M.Di Toro, P.Piattelli and P.Sapienza, Pag.31.

[7] A.Bonaccorso, Phys.Rev. C**C51**, 822 (1995).

[8] L.I.Shiff, *Quantum Mechanics*, Mc Graw-Hill Kogasha Ltd , Tokyo 1968, Pag. 44.

[9] J M.Cowley, *Diffraction Physics*, North-Holland Publishing Company, Amsterdam,Oxford, 1985.

[10] L.Lo Monaco and D.M.Brink, J.Phys.G **11**, 935 (1985).

[11] I.S. Gradshteyn and I.M.Ryzhik, *Table of Integrals, Series and Products*, Academic Press, New York, 1980. Pag.952.

[12] A.Messiah, *Mécanique Quantique*, Dunot, Paris, 1958. Vol.1, pag.415.

[13] Fl.Stancu and D.M.Brink, Phys.Rev. C**32**, 1937 (1985).

[14] A.Bonaccorso, G.Piccolo and D.M.Brink, Nucl.Phys. **A441**, 555 (1985).

[15] H.Sagawa, Phys.Lett. **B 286**, 7 (1992).

[16] L.D.Landau and E.M.Lifshitz, Quantum Mechanics, Pergamon Press London (1958), Ch. VII.

[17] C.L.Fink, B.L.Cohen,J.C. van der Weerd and R.J.Petty, Phys.Rev. **185**, 1568 (1969).

[18] O.F.Nemets, V.M.Pugach, M.V.Sokolov and B.G.Struzhko, in Proceedings of the International Symposium on Nuclear Structure, Dubna,USSR,1968, (unpublished).

[19] D.M.Brink, *Semiclassical Methods in Nucleus-Nucleus Scattering*, Cambridge University Press, Cambridge, 1985. Pag.19.

Figure Captions

Fig.1 Values of the parameter η from Eq.(2.5) for ^{11}Be solid line, and ^{10}Be dashed line.

Fig.2. Plot of the term $e^{-k_f^2 aR_2(\cos\theta - k_2/k_f)^2}$ and of the term $\frac{1}{\cosh(2k_f a\pi\sin\theta)-\cos(2\eta a\pi)}$ in Eq.(2.28) for the ^{11}Be breakup (solid line and dashed line respectively), and for the ^{10}Be breakup (dotdashed line and dotted line respectively), for a final neutron energy $\varepsilon_f = 40MeV$.

Fig.3. Momentum distribution for the $2s_{1/2}$ state in ^{11}Be, solid line, and $1p_{1/2}$-state in ^{10}Be, dashed line.

Fig.4. Angular distribution of the one-neutron breakup in the reactions $^9Be(^{11}Be,^{10}Be)^9Be + n$ solid line, and $^9Be(^{10}Be,^9Be)^9Be + n$ dotted line, at $E_{inc} = 41A.MeV$. The target potential parameters are those of Table II. Experimental points for the ^{11}Be-induced reaction are from [3].

Fig.5. The solid curve is the same as Fig.2 but now the dashed line is calculated with $a = 0.55fm$ and the dotted line with $a = 0.65fm$. a is the diffuseness parameter of the target Woods-Saxon potential.

Fig.6. Angle integrated energy spectra for ^{11}Be (solid line) and ^{10}Be projectile (dotted line).

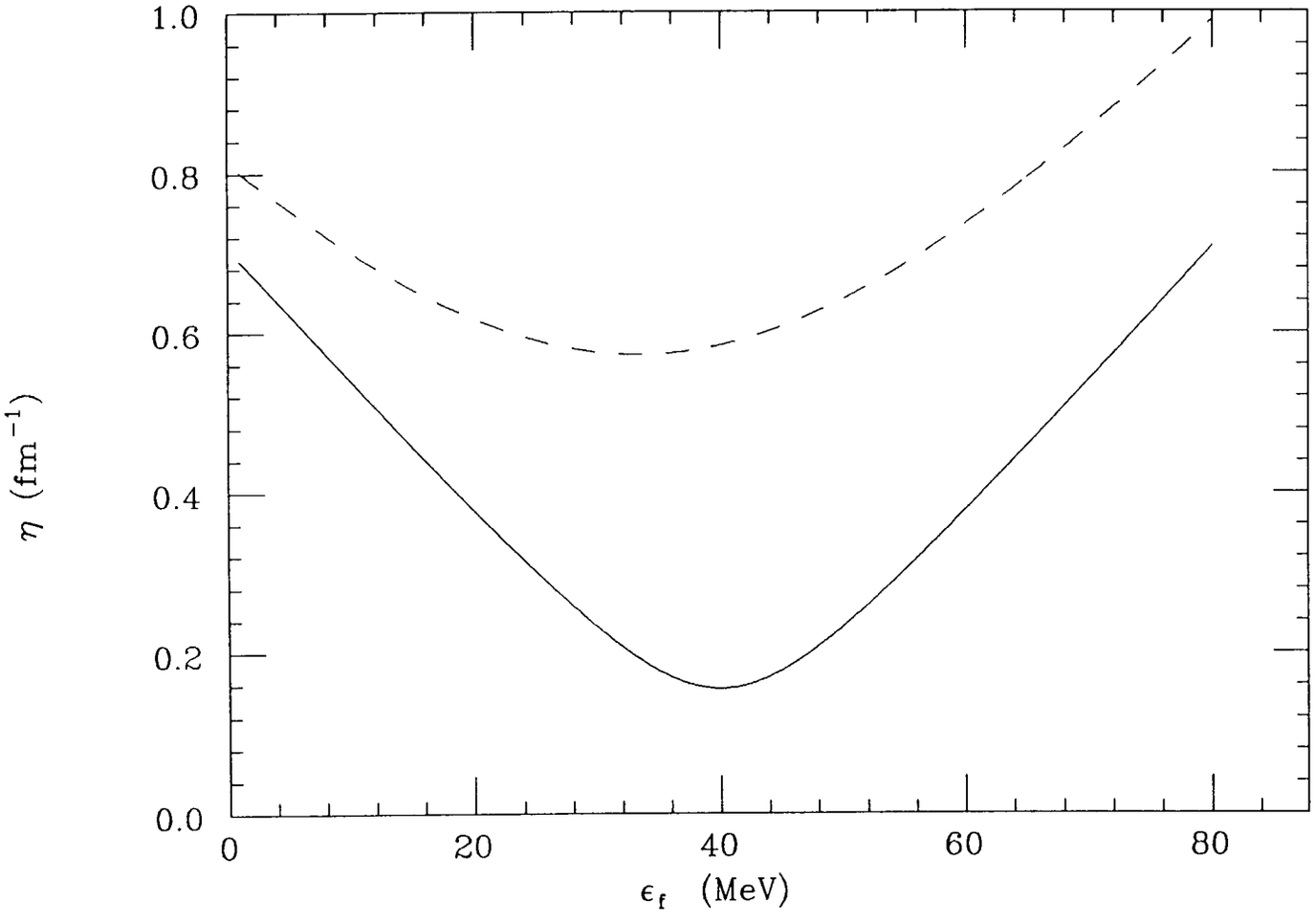

Fig. 1

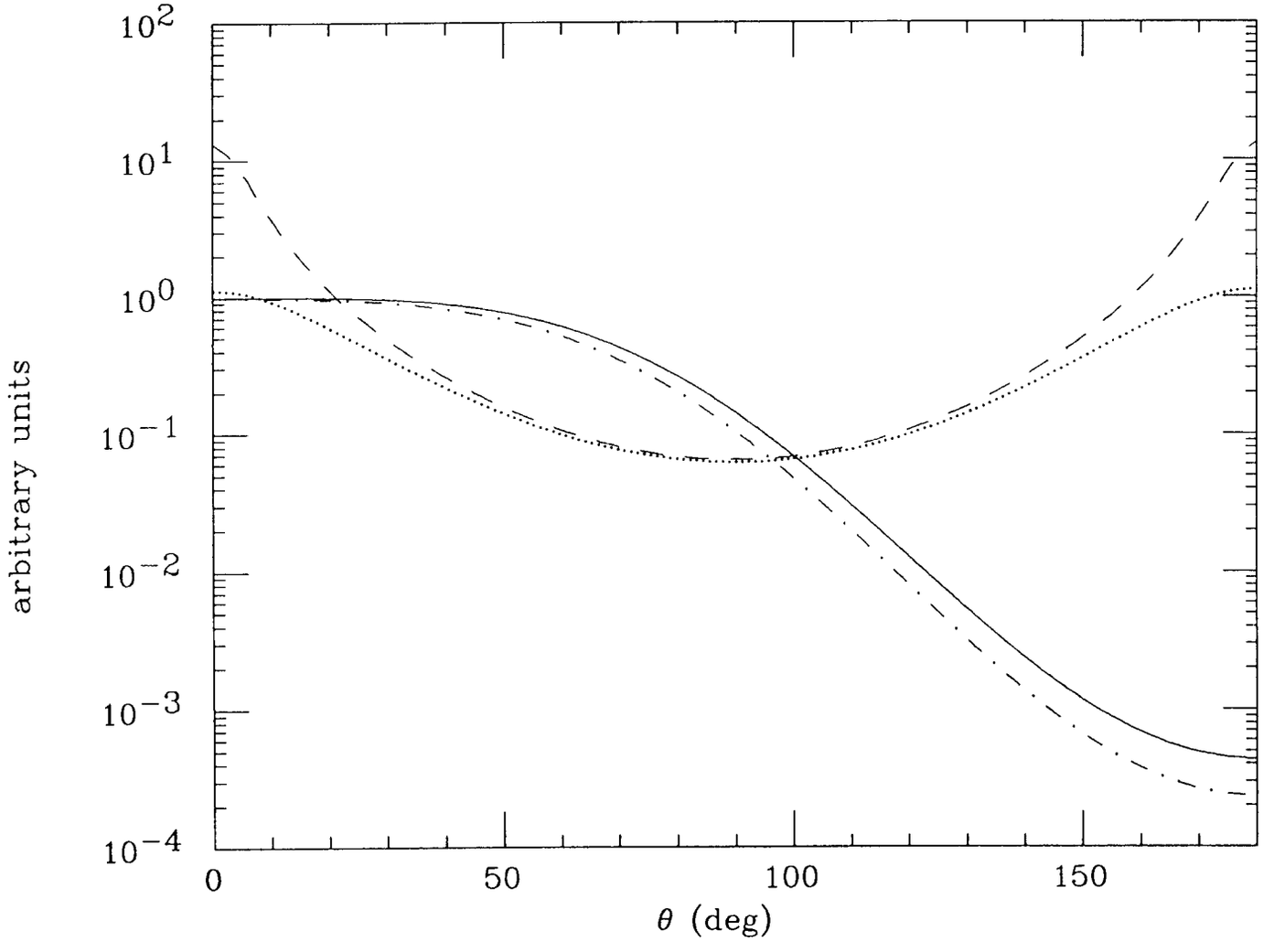
10^2
10^1
10^0
10^{-1}
10^{-2}
10^{-3}
10^{-4}
arbitrary units
0
50
100
150
θ (deg)

Fig. 2

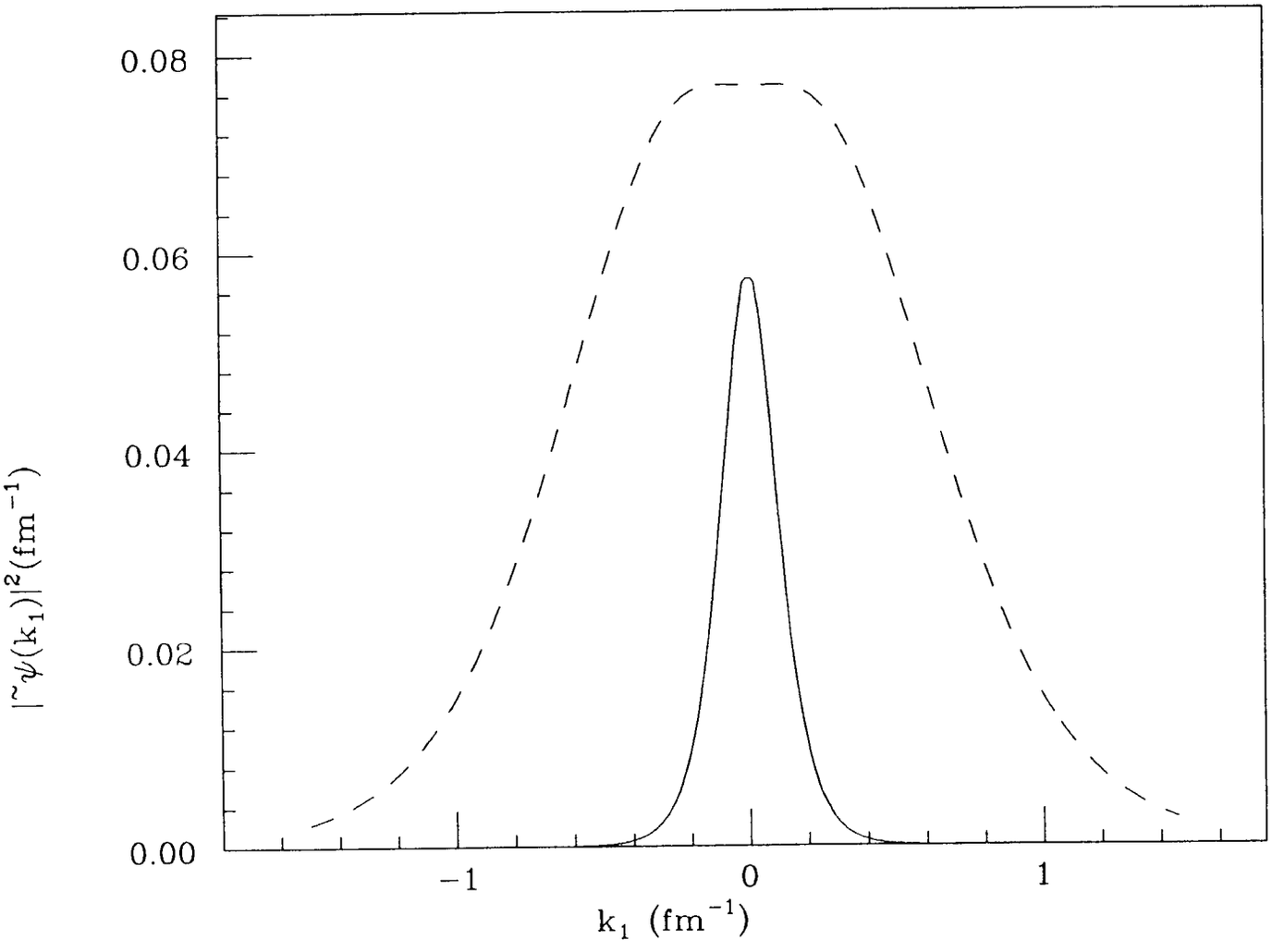

Fig. 3

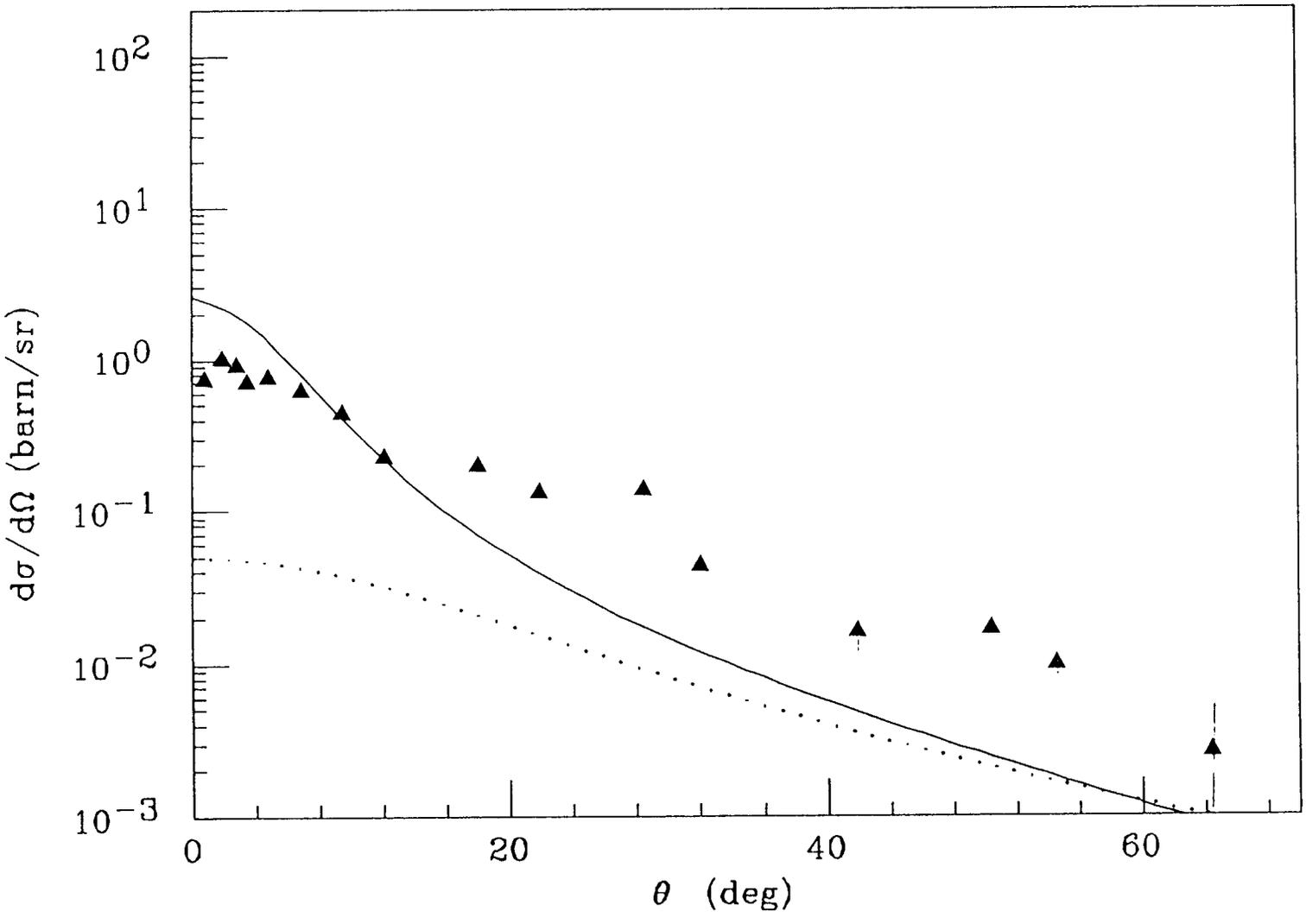
10^2
10^1
10^0
10^{-1}
10^{-2}
10^{-3}
$d\sigma/d\Omega$ (barn/sr)
0
20
40
60
θ (deg)

Fig 4

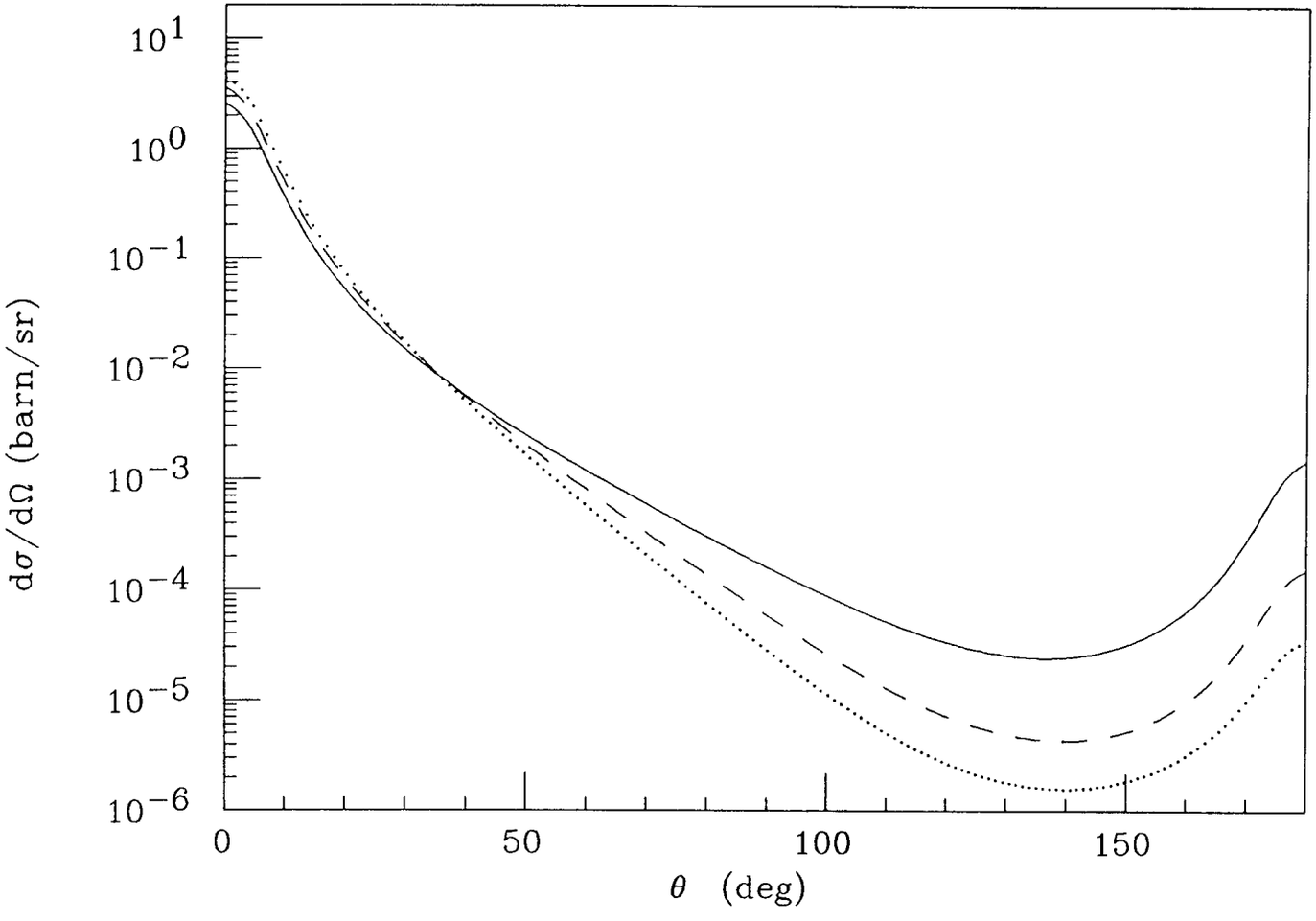
10^1
10^0
10^{-1}
10^{-2}
10^{-3}
10^{-4}
10^{-5}
10^{-6}
$d\sigma/d\Omega$ (barn/sr)
0
50
100
150
θ (deg)

Fig. 5

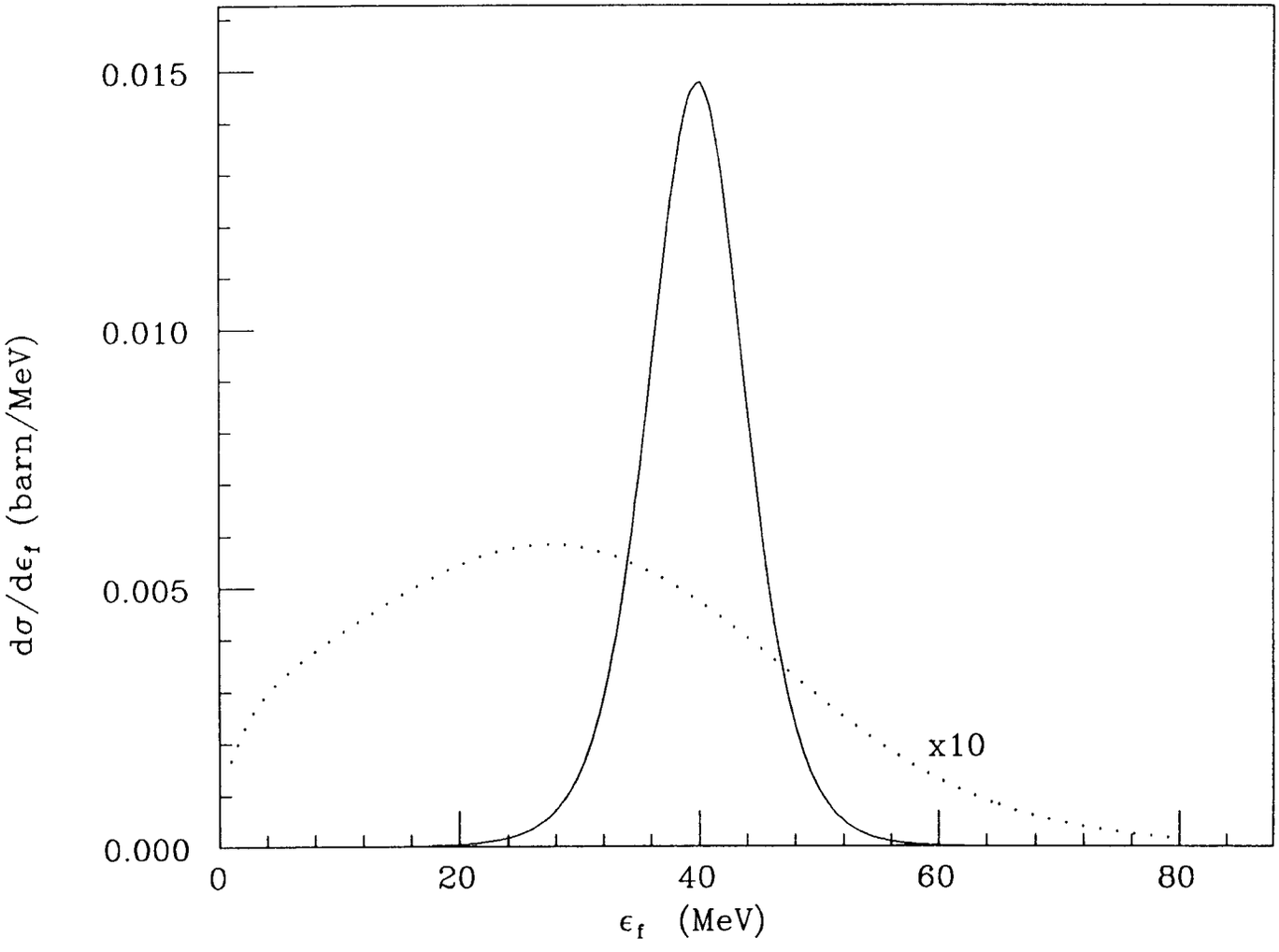
0.015
0.010
0.005
0.000
0
20
40
60
80
$d\sigma/d\epsilon_f$ (barn/MeV)
ϵ_f (MeV)
x10

Fig. 6